# Nanomechanics of Individual Carbon Nanotubes from Pyrolytically Grown Arrays

Ruiping Gao,[1,4] Zhong L. Wang,[1,*] Zhigang Bai,[1] Walter A. de Heer,[2] Liming Dai,[3] and Mei Gao[3]

[1]*School of Materials Science and Engineering, Georgia Institute of Technology, Atlanta, Georgia 30332-0245*
[2]*School of Physics, Georgia Institute of Technology, Atlanta, Georgia 30332-0430*
[3]*CSIRO Molecular Science, Private Bag 10, Clayton South MDC, Clayton 3169, Australia*
[4]*University of Science and Technology Beijing, Beijing, China*

The bending modulus of individual carbon nanotubes from aligned arrays grown by pyrolysis was measured by *in situ* electromechanical resonance in transmission electron microscopy (TEM). The bending modulus of nanotubes with point defects was $\sim$30 GPa and that of nanotubes with volume defect was 2–3 GPa. The time-decay constant of nanotube resonance in a vacuum of $10^{-4}$ Torr was $\sim$85 $\mu$s. A femtogram nanobalance was demonstrated based on nanotube resonance; it has the potential for measuring the mass of chain-structured large molecules. The *in situ* TEM provides a powerful approach towards nanomechanics of fiberlike nanomaterials with well-characterized defect structures.

PACS numbers: 81.05.Ys, 07.10.Lw, 81.05.Tp

Carbon nanotubes may have huge potential for future technology because of their superior electrical, mechanical, and chemical properties [1]. Characterizing the properties of *individual* carbon nanotubes requires novel techniques because the small size of the objects prohibits the applications of the well-established conventional tools. Several approaches have been developed for measuring the mechanical properties of a carbon nanotube. For example, the characteristic curve of the force vs the static displacement of one-end-fixed carbon nanotubes has been measured by atomic force microscopy [2]. Direct measurements of the bending arc of single-walled carbon nanotube ropes have been carried out by positioning the nanotubes across holes drilled on an alumina template while the tip pushed at the center to give the elastic and shear moduli [3]. A quantitative measurement of the amplitude of the thermally induced tip vibration at the free end of a carbon nanotube has also been achieved in transmission electron microscopy (TEM) [4]. An alternative method for characterizing the fluctuation of electron current as a result of thermally induced wire vibration was proposed by Osakabe *et al.* [5], which works only for large-size nanowires whose vibration frequency is on the order of a few thousands of Hertz. Also, a tensile testing apparatus has been constructed by Pan *et al.* [6] to measure the mechanical properties of ultralong carbon nanotubes ($\sim$2 mm in length). We recently invented a new method based on the electric-field-induced mechanical resonance in TEM that allows a direct measurement of the mechanical properties of a *single* carbon nanotube at high precision [7].

The ultrahigh mechanical strength of carbon nanotubes produced by arc discharge is due to their structural perfection and uniformity. For applications in flat panel display and composite materials, aligned carbon nanotube arrays produced by catalyst-assisted pyrolysis [8–10] are very attractive. From a structural point of view, carbon nanotubes produced by chemical synthesis are very different from those produced by arc discharge in that the former contain a higher density of point defects because of the introduction of pentagons and/or heptagons. The objective of this paper is to describe measurements of the mechanical properties of individual multiwalled carbon nanotubes, aiming at quantitatively determining the effect of growth defects on the bending modulus of carbon nanotubes.

The aligned carbon nanotubes were prepared by pyrolysis of iron (II) phthalocyanine, FePc, under $Ar/H_2$ atmosphere at a predetermined temperature using a quartz substitute in a flow reactor consisting of a quartz glass tube and a dual furnace fitted with independent temperature controllers, as reported in detail elsewhere [11]. From a piece of the scratched film [Fig. 1(a)], scanning tunneling microscopy (SEM) clearly reveals the high density of the aligned carbon nanotubes. To show the details of the carbon nanotubes, a small quantity of the as-grown film was dispersed in a holey carbon film supported by copper mesh, which was inserted in TEM for examination. The carbon nanotubes have an average length of $\sim$10 $\mu$m and an average diameter of $\sim$20 nm [Fig. 1(b)]. The body of the nanotubes can be attributed to a bamboolike structure [Fig. 1(c)]. The curly shape of the nanotube is due to the high density of point defects produced in the growth, by which we mean the existence of pentagonal and heptagonal carbon rings in the hexagonal networks.

It is crucial to observe the nanotube directly while its properties are being measured. To carry out the property measurement of a single nanotube with a well-characterized structure, a TEM specimen holder was specially built for applying a voltage across the nanotube and its counterelectrode [12,13]. The nanotubes were each fixed at one end to a gold/platinum wire, while the other end was close to a counterelectrode (gold ball) at a distance of a few microns. The forefront of the electrode with carbon nanotubes and the counterelectrode can be directly seen under TEM. Thus, the measurements can be done on a specific nanotube whose microstructure
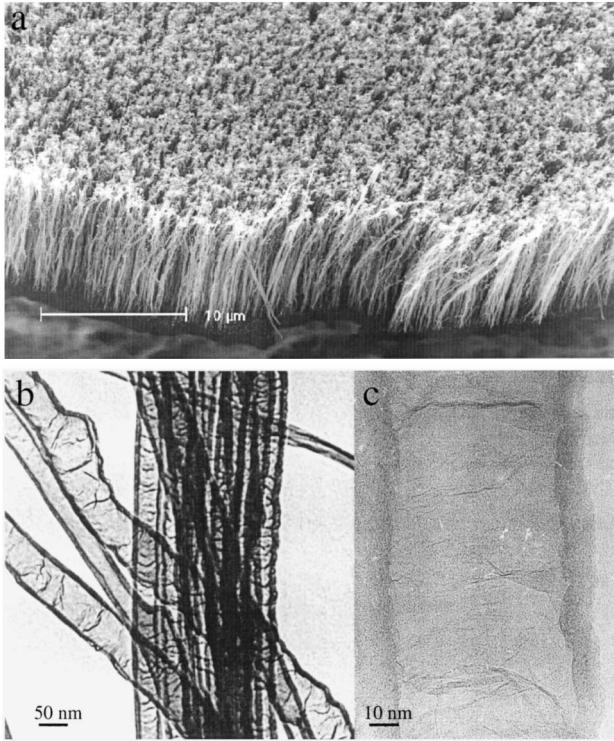
       

FIG. 1. (a) SEM image of the as-grown aligned carbon nanotube arrays on a quartz substrate. (b) Low-magnification TEM image showing the bamboolike structure of the carbon nanotubes. (c) A high-magnification TEM image showing the graphitic layered structures in the wall of a nanotube.

is determined by transmission electron imaging and diffraction. The TEM was operated at 100 kV using a JEOL 100C. This acceleration voltage produced no detectable radiation damage to the carbon nanotubes [7].

To measure the bending modulus of a carbon nanotube, an oscillating voltage with a tunable frequency is applied on the nanotube so that resonance can be induced by changing the frequency (Fig. 2). It is vital to identify the true base resonance frequency. Because of the difference between the surface work functions between the carbon nanotubes and the counter electrode (Hg or Au), a static charge exists even at zero applied voltage. Therefore, under an applied field the induced charge on the carbon nanotube can be represented by $Q = Q_0 + \alpha V_d \cos 2\pi \nu t$, where $Q_0$ represents the charge on the tip to balance the difference in surface work functions, $\alpha$ is a geometrical factor, and $V_d$ is the amplitude of the applied voltage. The force acting on the carbon nanotube is

$$
\begin{aligned}
F &= \beta(Q_0 + \alpha V_d \cos 2\pi \nu t)^2 \\
&= \beta Q_0^2 + \alpha^2 \beta V_d^2/2 + 2\alpha \beta Q_0 V_d \cos 2\pi \nu t \\
&\quad + \alpha^2 \beta V_d^2/2 \cos 4\pi \nu t,
\end{aligned}
\tag{1}
$$

where $\beta$ is a proportional constant. Thus, resonance can be induced at $\nu$ and $2\nu$ with vibration amplitudes proportional to $V_d$ and $V_d^2$, respectively. The former is a linear term in which the resonance frequency equals the applied frequency, while the latter is a nonlinear term and the
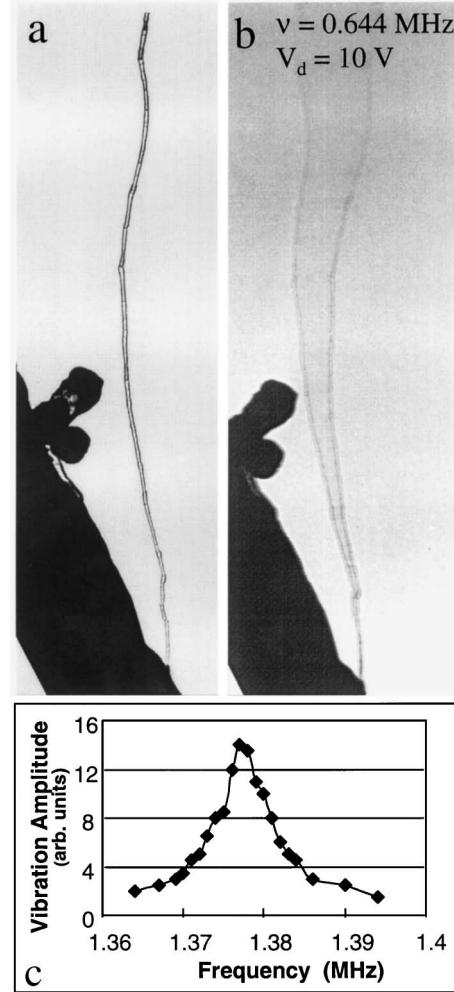


FIG. 2. A carbon nanotube at (a) the stationary and (b) the first resonance mode. (c) The FWHM of the resonance peak measured from another nanotube. The resonance occurs at 1.378 MHz.

resonance frequency is twice the applied frequency. In practical experiments, the linear and nonlinear terms have been distinguished by observing the dependence of the vibration amplitude on the magnitude of the voltage $V_d$. In order to determine if an observed frequency is the true base frequency, one needs to examine the resonance at a frequency that is half, or close to half, of the observed resonance frequency to ensure that no resonance is occurring.

The natural resonance frequency of a nanotube depends on the tube outer diameter ($D$), inner diameter ($D_1$), the length ($L$), the density ($\rho$), and the bending modulus ($E_b$) of the nanotube. For a tube with uniform structural and mass distribution, the classical elasticity theory gives the resonance frequency [14]

$$
\nu_i = \frac{\beta_i^2}{8\pi} \frac{1}{L^2} \sqrt{\frac{(D^2 + D_1^2)E_b}{\rho}},
\tag{2}
$$

where $\beta_1 = 1.875$ and $4.694$ for the first and the second harmonics, respectively. Equation (2) may be applicable to the nanotubes used in this study if the distribution of point

defects is approximately uniform along the nanotube. If the structure presented in Fig. 1(b), after removing the iron particles, can be approximated as a uniform tube structure, the bending modulus of the tube can be calculated using Eq. (2) based on the experimentally measured data. The experimental results are summarized in Table I. One critical condition that Eq. (2) holds is that the fixed end of the nanotube is rigid. In practice, if the root was slightly loose, the resonance frequency would shift as vibration proceeds. We have carefully checked the stability of the resonance frequency to ensure its time independence.

We have previously reported the bending modulus of carbon nanotubes produced by arc discharge [7]. For nanotubes with an outer diameter larger than 30 nm, the bending modulus is ~200 GPa. This value is much higher than those shown in Table I for the nanotubes produced by pyrolysis. The softening of the nanotube in the current case is attributed to defects, mainly point defects, present in the nanotube.

The FWHM of the resonance peak of a carbon nanotube was determined by observing the dependence of the vibration amplitude on the frequency of the applied electric field, as shown in Fig. 2(c). The ratio between the FWHM to the resonance frequency is $\Delta\nu/\nu_1 = 0.6\%-0.7\%$. This value remains the same for several carbon nanotubes with different lengths, diameters, and defect density. It is almost identical to the value measured under the same experimental conditions for the nanotubes produced by arc discharge [7]. However, the measurement in the atmosphere under an optical microscope indicated that the ratio of $\Delta\nu/\nu_1$ is much larger than that in vacuum [14].

To explore the intrinsic meaning of the measured $\Delta\nu/\nu_1$ value, we consider a one-dimensional harmonic oscillator with an intrinsic resonance frequency $\nu_1$. If a viscosity (or friction) force acts on the particle and the force is proportional to the instantaneous speed of the particle, the damping of the vibration amplitude is given by $\exp(-t/\tau_0)$, where $\tau_0$ is the life-decay constant of the oscillator. This decay constant is related to $\Delta\nu/\nu_1$ by Eq. (3) for $\Delta\nu/\nu_1 \ll 1$,

$$\tau_0 = [(\Delta\nu/\nu_1)\pi\nu_1/1.732]^{-1}. \qquad (3)$$

For $\Delta\nu/\nu_1 = 0.65\%$, $\nu_1 = 1.0$ MHz, the lifetime is $\tau_0 = 85$ $\mu$s. From the definition of $\tau_0$, the viscosity/friction coefficient $\eta = 2M/\tau_0$, where $M$ is the mass of the particle.

Thus, the time decay constant depends mainly on the viscosity coefficient of the nanotube in vacuum ($10^{-4}$ Torr) under which the measurement was made, and it is almost independent of the intrinsic structure of the carbon nanotube. This agrees with our experimental observation, and Eq. (3) can also be used to explain the larger value of $\Delta\nu/\nu_1$ obtained in air than that obtained in vacuum, given that the atmosphere should have a higher viscosity (friction) coefficient.

To trace the sensitivity of resonance frequency on beam illumination and radiation damage at 100 kV, a carbon nanotube was set on resonance for more than 60 min at 0.7152 MHz and at a vibration angle of ~40°. Two important facts were observed. While the nanotube was set on resonance for $2.575 \times 10^9$ cycles, its structure was still intact and no visible change was observed. This clearly showed the superior creeping properties of the carbon nanotube. The resonance frequency showed almost no drift during the observation, suggesting its superior structural stability.

Carbon nanotubes produced by pyrolysis usually have not only a high density of point defects but also volume defects. Figure 3 shows a TEM image of a nanotube that exhibits a neck structure at the middle of its body. From the vibration shape of the nanotube, there is no abrupt change at the defect point and the vibration curve is smooth. We have examined the electrostatic deflection of the nanotube when a constant voltage is applied across the electrodes. The nanotube showed a smooth deflection without visible change in its shape near the volume defect. Therefore, the volume defect does not seem to introduce any significant softening at the local region, due, most probably, to the collectively rippling deformation on the inner arc of the bent nanotube [7]; the vibration of the entire system could still be described by the elastic theory. If Eq. (2) is still applicable to this case, resonance measurement shows that the bending modulus of the tube is 2.2 GPa, about 15 times smaller than the other tubes. Another tube with a similar structure has a modulus of 5.0 GPa.

In analogy to a pendulum, the mass of a particle attached at the end of the nanotube could significantly affect the resonance frequency, through which we can derive the mass of the particle. This is the principle of the "femtogram nanobalance" presented here. Figure 4(a) shows a carbon nanotube that is attached to the body of another

TABLE I. Bending modulus of carbon nanotubes produced by pyrolysis.

| Nanotube | Outer diameter $D$ (nm) ($\pm 1$) | Inner diameter $D_1$ (nm) ($\pm 1$) | Length $L$ ($\mu$m) ($\pm 0.05$) | Frequency $\nu$ (MHz) | $E_b$ (GPa) |
|---|---|---|---|---|---|
| 1 | 33 | 18.8 | 5.5 | 0.658 | $32 \pm 3.6$ |
| 2 | 39 | 19.4 | 5.7 | 0.644 | $26.5 \pm 3.1$ |
| 3 | 39 | 13.8 | 5 | 0.791 | $26.3 \pm 3.1$ |
| 4 | 45.8 | 16.7 | 5.3 | 0.908 | $31.5 \pm 3.5$ |
| 5 | 50 | 27.1 | 4.6 | 1.420 | $32.1 \pm 3.5$ |
| 6 | 64 | 27.8 | 5.7 | 0.968 | $23 \pm 2.7$ |
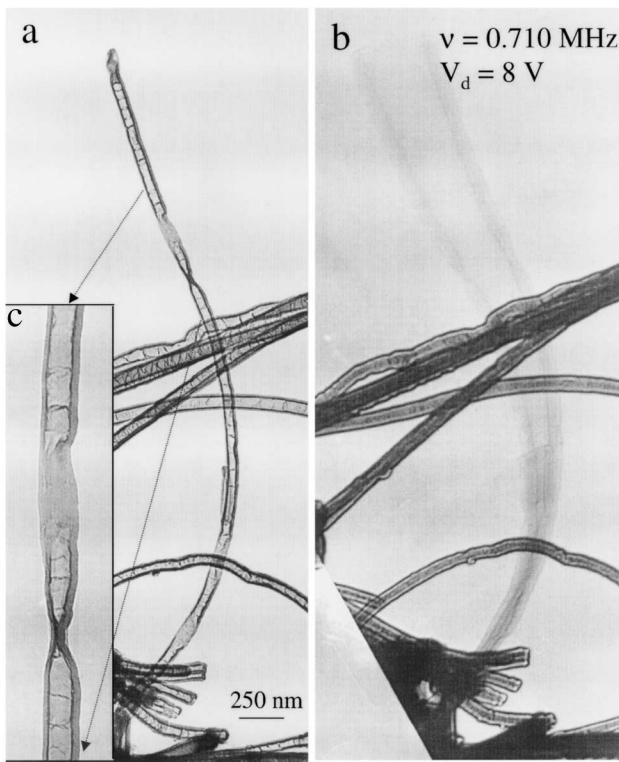
FIG. 3. A carbon nanotube at (a) the stationary and (b) the first resonance mode; (c) shows the presence of a necklike volume defect along the body of the nanotube.
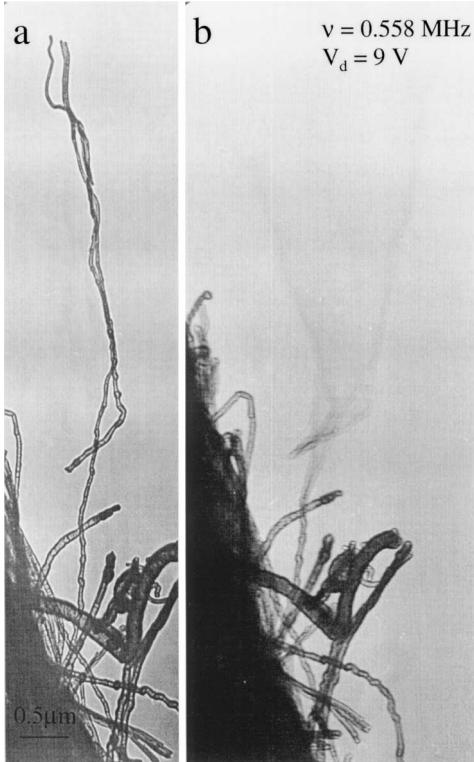


FIG. 4. (a) The stationary and (b) the first resonance mode of a carbon nanotube with another nanotube around its body. This is the principle of femtogram nanobalance of chain-structured large molecules.

nanotube. The latter is directly affixed to the substrate. Resonance of the system occurs at 0.5598 MHz. If $E_b = 30$ GPa from the data given in Table I, a simple calculation using the effective mass shows that the mass of the attached nanotube is $\sim 23$ fg (1 fg $= 10^{-15}$ g). Theoretical calculation for a straight graphite tube gives 17 fg. This is *the most sensitive and smallest balance in the world,* which could be used to measure the mass of chain-structured large molecules.

In summary, the bending modulus of carbon nanotubes produced by pyrolysis is about 10 times smaller than the nanotubes produced by arc discharge. This difference is attributed to the effect of point defects present in the nanotubes. The *in situ* TEM technique demonstrated here is a new approach towards nanomechanics, which allows the structure and property of individual nanotubes to be correlated, providing a powerful technique for investigating the mechanical properties of fiberlike nanomaterials with well-characterized structural defects.

*Corresponding author.
Electronic address: zhong.wang@mse.gatech.edu

[1] See, for example, R. Saito, G. Dresselhaus, and M. S. Dresselhaus, *Physical Properties of Carbon Nanotubes* (Imperial College Press, London, 1998).
[2] E. W. Wong, P. E. Sheehan, and C. M. Lieber, Science **277**, 1971 (1997).
[3] J-P Salvetat, G. A. D. Briggs, J.-M. Bonard, R. R. Bacsa, A. J. Kulik, T. Stockli, N. A. Burnham, and L. Forro, Phys. Rev. Lett. **82**, 944 (1999).
[4] M. M. Treacy, T. W. Ebbesen, and J. M. Gibson, Nature (London) **38**, 678 (1996).
[5] N. Osakabe, K. Harada, M. I. Lutwyche, H. Kasai, and A. Tonomura, Appl. Phys. Lett. **70**, 940 (1997).
[6] Z. W. Pan, S. S. Xie, L. Lu, B. H. Chang, L. F. Sun, W. Y. Zhou, G. Wang, and D. L. Zhang, Appl. Phys. Lett. **74**, 3152 (1999).
[7] P. Poncharal, Z. L. Wang, D. Ugarte, and W. A. de Heer, Science **283**, 1513 (1999).
[8] W. Z. Li, S. S. Xie, L. X. Qian, B. H. Chang, B. S. Zou, W. Y. Zhou, R. A. Zhao, and G. Wang, Science **274**, 1701 (1996).
[9] Z. F. Ren, Z. P. Huang, J. H. Xu, P. B. Wang, M. P. Siegal, and P. N. Provencio, Science **282**, 1105 (1998).
[10] S. S. Fan, M. G. Chapline, N. R. Franklin, T. W. Tombler, A. M. Cassell, and H. J. Dai, Science **283**, 512 (1999).
[11] S. M. Huang, L. M. Dai, and A. W. H. Mau, J. Phys. Chem. B **103**, 4223 (1999).
[12] Z. L. Wang, P. Poncharal, and W. A. de Heer, Pure Appl. Chem. **72**, 209 (2000).
[13] Z. L. Wang, P. Poncharal, and W. A. de Heer, Microsc. Microanal. Microstruct. **6**, 224 (2000).
[14] L. Meirovich, *Elements of Vibration Analysis* (McGraw-Hill, New York, 1986).